Electronic Supplementary Information

A chemical-electrochemical cascading strategy for the efficient synthesis of 2,5-furandicarboxylic acid and its methyl ester from 2-furoic acid and CO_2

Ruizhi Li, Minling Zhong, Maitreyo Biswas, Nan Jiang, Arun Mannodi-Kanakkithodi, and Yujie Sun

Experimental section

Chemicals and materials

Tetrabutylammonium bromide (TBABr, 98%), Methyl 5-bromofuran-2-carboxylate (MBFC, 98%), Methyl-2-furoate (MF, 98.91%), Dimethyl furan-2,5-dicarboxylate (99.92%), were purchased from Ambeed, Inc. Sodium hydroxide was purchased from Aldon, Inc. Silver nanopowder (<100 nm particle size, 99.5%), Methanol (MeOH, ≥99.9%), Acetonitrile (MeCN, ≥99.9%), N,N-Dimethylformamide (DMF, ≥99.9%) were purchased from Sigma-Aldrich. Single-crystal surfaces of Ag (111), Ag (110), and Ag (100) were purchased from Hefei Kejing Materials Technology Co., Ltd. 5-(methoxycarbonyl)furan-2-carboxylic acid (MFCA) was synthesized according to the reported literature with slight modifications.[1] All reagents in this work were purchased and used without further purification. Deionized water was used throughout the experiments.

Preparation of catalysts

The Ag electrodes were prepared using a standard air-brush technique. Briefly, Ag nanoparticles (40 mg) were dispersed in 4 mL of isopropanol and sonicated for 30 minutes to form a uniform catalyst ink. The ink was then air-brushed onto carbon paper (Sigracet GDL 39BB, Fuel Cell Store) to achieve a catalyst loading of ~0.8 mg cm^{-2}. The effective geometric area of the electrode was 1.0 cm^2. Other electrodes were fabricated following the same procedure to ensure uniformity. The Ag on glassy carbon electrode was prepared via electrodeposition using a standard three-electrode setup on a VMP-3 potentiostat (BioLogic Science Instruments). A polished glassy carbon electrode served as the working electrode, with an Ag/AgCl reference electrode (saturated KCl aqueous electrolyte) and a Pt mesh counter electrode. Electrodeposition was carried out at -0.2 V vs. Ag/AgCl in an aqueous solution containing 25 mM $AgNO_3$. The electrodeposition was terminated after passing a total charge of 1.5 C.

Materials characterization

The morphological features of the samples were characterized by scanning electron microscopy (SEM, FEI XL30) operated at 15 kV. X-ray diffraction (XRD) patterns were recorded using a Philips X'Pert Pro PW3040/00 (PANalytical) diffractometer with Cu Kα radiation (λ = 1.5406 Å), operated at 45 kV and 40 mA. Scans were collected over a 2θ range of 10° to 90°. ^{1}H NMR and ^{13}C NMR spectra were recorded in the designated solvents on a Bruker AV 500 MHz spectrometer.

Electrochemical measurements

All electrocatalytic measurements were performed using a VMP-3 potentiostat (Biological Science Instruments) in a two-compartment H-cell separated by an organic anion exchange membrane (Fumasep FAB-PK-130), with a Pt mesh counter electrode and a leakless Ag/AgCl reference electrode (eDAQ). Prior to each electrocatalytic measurement, MeCN or DMF was freshly obtained from a solvent purification system (Mbraun, Inc.) and used without further treatment. CV measurements were carried out in a one-compartment, three-electrode cell by using Ag-decorated glassy carbon electrode as the working electrode performed at a scan rate of 20 mV s^{-1}. LSV measurements were performed in a two-compartment, three-electrode cell with an Ag/CP working electrode at a scan rate of 10 mV s^{-1}, without iR compensation. Under standard conditions, the

catholyte consisted of 0.1 M TBABr and 5 mM MBFC in MeCN, while the anolyte contained 0.1 M TBABr in MeCN. CO_2 was continuously purged into the electrolyte during electrolysis and was first passed through a Drierite drying tube to remove moisture prior to entering the cell.

In situ ATR-FTIR

In situ attenuated total reflection Fourier transform infrared (ATR-FTIR) spectroscopy was performed using a Bruker INVENIO FT-IR spectrometer equipped with a liquid nitrogen-cooled LN-MCT detector at a resolution of 4 cm^{-1} and 64 scans per spectrum. A micro-ATR accessory with a Si crystal was employed to enable small-area sample measurements. The Ag catalyst ink was dropped-cast directly onto an Au-coated Si internal reflection element, which served as the working electrode. A leakless Ag/AgCl reference electrode and a Pt mesh counter electrode were used (Figure S15). The electrolyte consisted of 5 mM MBFC and 0.1 M TBABr in MeCN and was saturated with CO_2 for 30 minutes prior to measurements. Before data acquisition, the spectrometer was purged with Ar for 30 minutes to remove atmospheric CO_2 and moisture. Electrochemical control of the potential and electrolysis time was maintained using a CHI 760E potentiostat.

Product quantification

Product quantification was performed using high-performance liquid chromatography (HPLC). After electrolysis, the electrolyte was acidified with 1.5 M HCl, and a 10 µL aliquot was diluted with 990 µL of deionized water. The resulting solution was analyzed using an Agilent 1260 Infinity HPLC system equipped with a C18 column and a UV-vis detector set at 265 nm. The mobile phase consisted of 5 mM ammonium acetate in water (35%) and acetonitrile (65%), delivered at a flow rate of 0.5 mL min^{-1} at room temperature.

The yield (%) of the electroreduction products were calculated based on the following equation:

$$\text{Yield (\%)} = \frac{\text{mole of product formed}}{\text{mole of initial substrate}} \times 100\%$$

The Faradaic efficiency (%) of the electroreduction products were calculated based on the following equation:

$$\text{FE (\%)} = \frac{\text{nF} \times \text{N}}{Q\text{total charge passed}} \times 100\%$$

where n is the number of electrons transferred for each product molecule, F is Faraday's constant (96,485 C mol^{-1}), N is the mole number of products and Q is the total passed charge. Notably, since the theoretical charge was fully passed in each electrolysis experiment, the obtained yield directly corresponds to FE.

The selectivity (%) of the electro-reduction products was calculated based on the following equation:

$$\text{Selectivity (\%)} = \frac{\text{mole of product formed}}{\text{mole of consumed substrate}} \times 100\%$$

Computational details

DFT computations were carried out to provide insights into the energy barriers of the debromination reaction of MBFC molecule on different Ag facets. All calculations were performed using the Vienna ab initio simulation package (VASP),[2] employing the projector augmented wave (PAW)[3,4] pseudopotentials. The surface energies for the slabs were calculated using the Generalized Gradient Approximation (GGA)-based Perdew–Burke–Ernzerhof (PBE)[5] revised functional for solids (PBEsol)[6] and corresponding adsorption calculations were performed using

GGA-PBE+D3 to include the empirical van der Waals interactions. A kinetic energy cutoff of 500 eV was set for the plane wave basis set with the convergence criteria set to 10^{-5} eV for energy and -0.01 eV/ $Å^{-1}$ for forces. The energy barriers for the debromination reaction were calculated using the Cl-NEB (climbing image nudged elastic band) method[7] with 9 intermediate images to resolve the minimum energy pathway (MEP) in Ag-311 and Ag-111 facets.

The Cl-NEB calculation was performed both in vacuum using standard VASP and in the MeCN solvation medium using the VASPsol++[8] package developed by the Plaisance group. VASPsol++ is a continuum solvation framework integrated with standard VASP that enables density functional theory calculations in the presence of a solvation medium. It incorporates nonlinear dielectric and ionic responses with a nonlocal cavity model, allowing a realistic treatment of electrochemical environments at only modest additional computational cost. The energy convergence criteria for electronic self-consistency in both VASP and VASPsol++ were set to 10^{-5} eV, while the forces on each atom were converged to -0.01 eV $Å^{-1}$ along with two extra electrons added as uniform electron density. For the VASPsol simulations, we used the nonlocal and nonlinear solvation model with the bulk dielectric constant of 37.5 for the MeCN medium. We initially performed single-point VASPsol calculations for all four facets (Figures S23-S26) followed by full scale Cl-NEB for the Ag (311) and Ag (111) facets (Figure 5).

Synthesis of methyl 2-furoate (MF)

2-Furoic acid (0.56 g, 5.0 mmol) was dissolved in methanol (12.5 mL), and concentrated H_2SO_4 (0.25 mL, 4.6 mmol) was added dropwise with stirring. The reaction mixture was refluxed for 12 h, then cooled to room temperature. Methanol was removed under reduced pressure, and the residue was extracted with ethyl acetate (3 × 10 mL). The combined organic layers were washed with saturated $NaHCO_3$ solution, dried over anhydrous Na_2SO_4, and concentrated under reduced pressure. The product, methyl 2-furoate, was obtained as a colorless liquid (0.57 g, 90% yield).

^{1}H NMR (400 MHz, DMSO-d_6) δ 8.00 – 7.94 (m, 1H), 7.31 (d, J = 3.5 Hz, 1H), 6.69 (dd, J = 3.5, 1.7 Hz, 1H), 3.80 (s, 3H) ppm.

^{13}C NMR (101 MHz, DMSO-d_6) δ 158.75, 148.02, 144.11, 118.75, 112.70, 52.14 ppm.

Synthesis of methyl 5-bromofuran-2-carboxylate (MBFC)

Methyl 2-furoate (1.26 g, 10.0 mmol) was dissolved in glacial acetic acid (20 mL) and heated to 60 °C. Bromine (0.9 mL, 18.0 mmol) was added dropwise in three equal portions (0.3 mL each) at 12 h intervals, and the reaction mixture was stirred at 60 °C for a total of 36 h. The reaction progress was monitored by TLC (hexane/ethyl acetate = 10:1, product R_f = 0.38). After completion, the mixture was cooled to room temperature, and a saturated aqueous $NaHSO_3$ solution was added until the color disappeared. The reaction mixture was extracted with ethyl acetate (3 × 20 mL). The combined organic layers were washed with saturated $NaHCO_3$ solution, dried over anhydrous Na_2SO_4, and concentrated under reduced pressure. The crude product was purified by silica gel column chromatography using hexane as the eluent to afford methyl 5-bromofuran-2-carboxylate as a white solid (1.57 g, 77% yield).

^{1}H NMR (400 MHz, DMSO-d_6) δ 7.36 (d, J = 3.6 Hz, 1H), 6.85 (d, J = 3.6 Hz, 1H), 3.81 (s, 3H) ppm.

^{13}C NMR (101 MHz, DMSO-d_6) δ 157.33, 145.57, 127.56, 120.77, 114.62, 52.03 ppm.

Synthesis of 5-(Methoxycarbonyl)furan-2-carboxylic acid (MFCA)

Furan-2,5-dimethyl carboxylate (FDME, 0.01 mol) and NaOH (0.013 mol) were each dissolved separately in methanol (20 mL and 10 mL, respectively). The NaOH solution was then added dropwise to the ester solution over 4 h at 50 °C using a syringe pump. After completion, the reaction mixture was acidified and cooled in an ice bath to induce precipitation. The resulting precipitate was filtered to afford MFCA as a white solid in near-quantitative yield.
^{1}H NMR (500 MHz, Methanol-d_4) δ 7.29 (d, J = 3.7 Hz, 1H), 7.26 (d, J = 3.5 Hz, 1H), 3.91 (s, 4H) ppm.
^{13}C NMR (126 MHz, Methanol-d_4) δ 160.76, 159.93, 148.96, 147.90, 119.64, 119.40, 52.76 ppm.

Post-electrolysis workup and isolation of FDCA
Electrolyte solutions collected from multiple electrolysis experiments (200 mL in total) were combined and acidified for HPLC analysis, which indicated an MFCA concentration of 5.2 mM. Volatile components were removed under reduced pressure, and the resulting residue was dissolved in 20 mL of 2 M aqueous NaOH. The alkaline mixture was extracted with ethyl acetate (3 × 20 mL) to remove the supporting electrolyte TBABr. During this basic workup step, the initially formed 5-(methoxycarbonyl)-2-furoic acid (MFCA) underwent hydrolysis under alkaline conditions, thus converting the product into 2,5-furandicarboxylic acid (FDCA). The aqueous phase was subsequently acidified to pH 4 with 2 M HCl and extracted with ethyl acetate (3 × 20 mL) to recover the organic product. The combined organic layers were dried over anhydrous Na_2SO_4, filtered, and concentrated under reduced pressure. The obtained solid was washed thoroughly with water, collected by filtration, and rinsed with a small amount of cold methanol. After drying under vacuum, 2,5-furandicarboxylic acid (FDCA) was isolated as a white powder (152 mg, 93.8% isolated yield).

Synthesis of 2,5-furandicarboxylic acid (FDCA)
A mixture of 0.2 g of 5-(Methoxycarbonyl)furan-2-carboxylic acid, 0.15 g KOH, 5 mL of methanol and 5 mL of distilled water was refluxed at 80 °C for 4 hours. After completion, the reaction mixture was acidified and cooled in an ice bath to induce precipitation. The precipitate was collected by filtration, washed three times with ice water and twice with ethanol, and dried in an oven at 60 °C overnight. The product, 2,5-furandicarboxylic acid, was obtained as a white solid (0.14 g, 76% yield).
^{1}H NMR (400 MHz, DMSO-d_6) δ 7.30 (s, 2H) ppm.
^{13}C NMR (101 MHz, DMSO-d_6) δ 158.86, 146.99, 118.36 ppm.

Synthesis of furan-2,5-dimethyl carboxylate (FDME)
5-(Methoxycarbonyl)furan-2-carboxylic acid (0.20 g, 1.18 mmol) was dissolved in methanol (12.0 mL), and concentrated H_2SO_4 (0.25 mL, 4.6 mmol) was added dropwise with stirring. The reaction mixture was refluxed for 12 h, then cooled to room temperature. Methanol was removed under reduced pressure, and the residue was extracted with ethyl acetate (3 × 10 mL). The combined organic layers were washed with saturated $NaHCO_3$ solution, dried over anhydrous Na_2SO_4, and concentrated under reduced pressure. The product, dimethyl 2,5-furandicarboxylate, was obtained as a white solid (0.16 g, 71% yield).
^{1}H NMR (500 MHz, DMSO-d_6) δ 7.44 (s, 2H), 3.86 (s, 6H) ppm.
^{13}C NMR (101 MHz, DMSO-d_6) δ 158.32, 146.50, 119.52, 52.87 ppm.

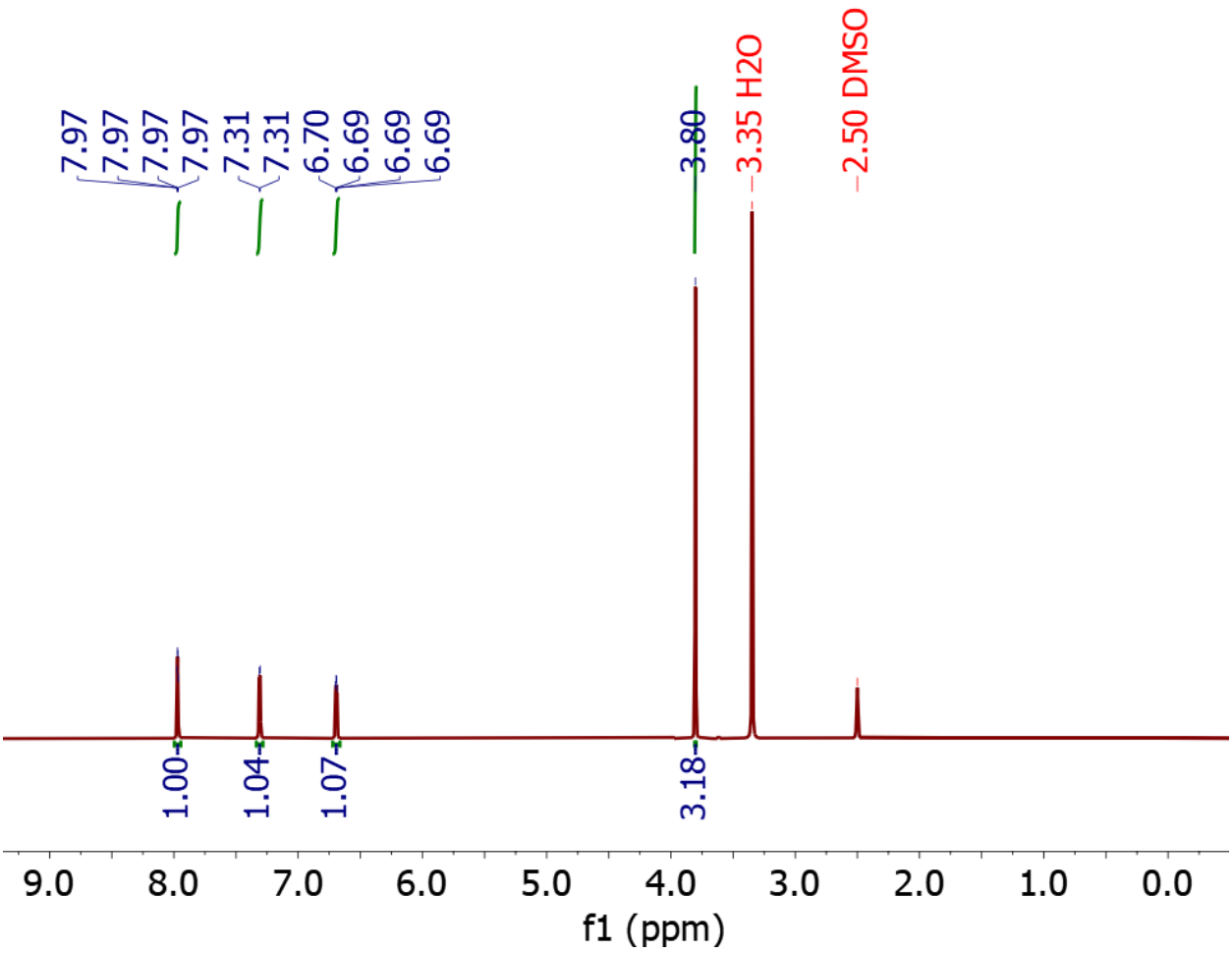

Figure S1. ^{1}H NMR spectrum of synthesized MF in DMSO-d_6.

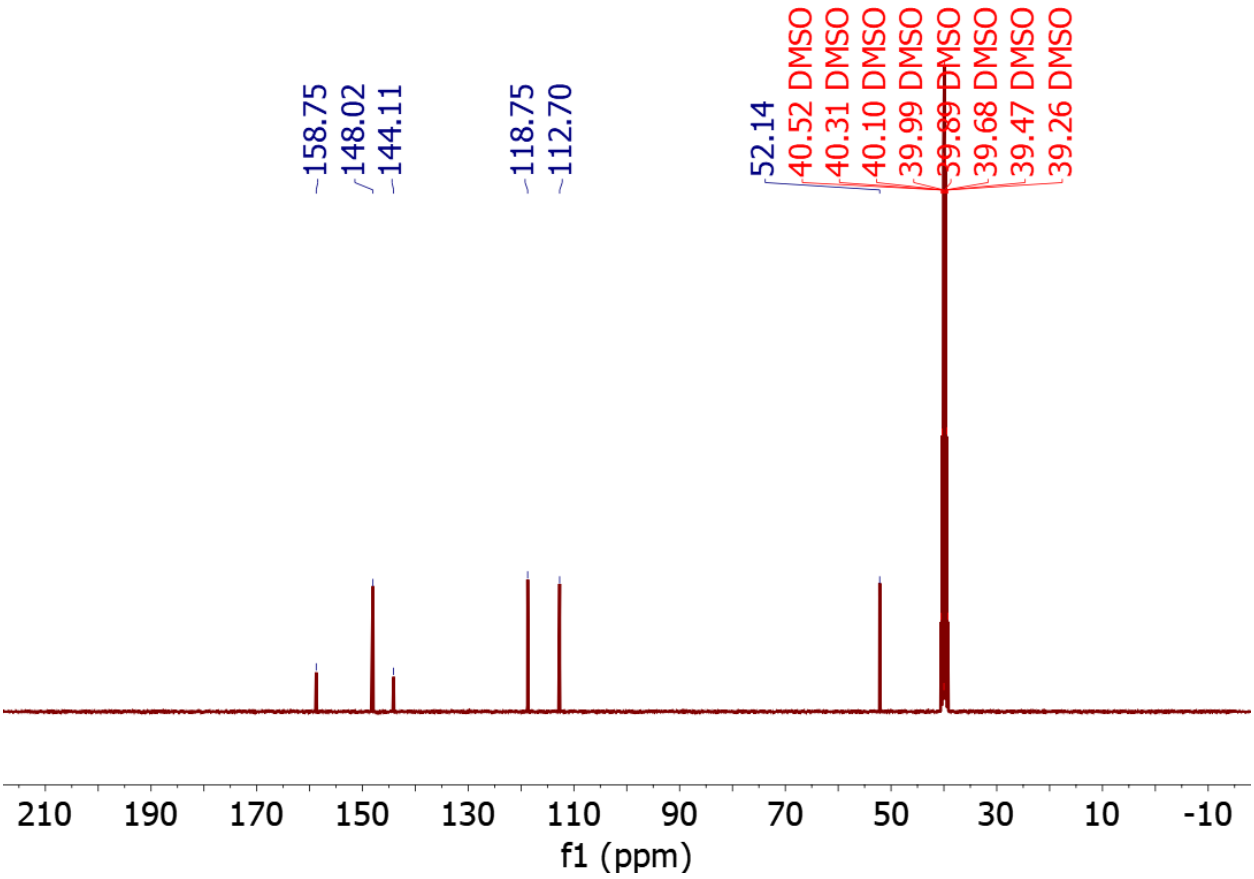

Figure S2. ^{13}C NMR spectrum of synthesized MF in DMSO-d_6.

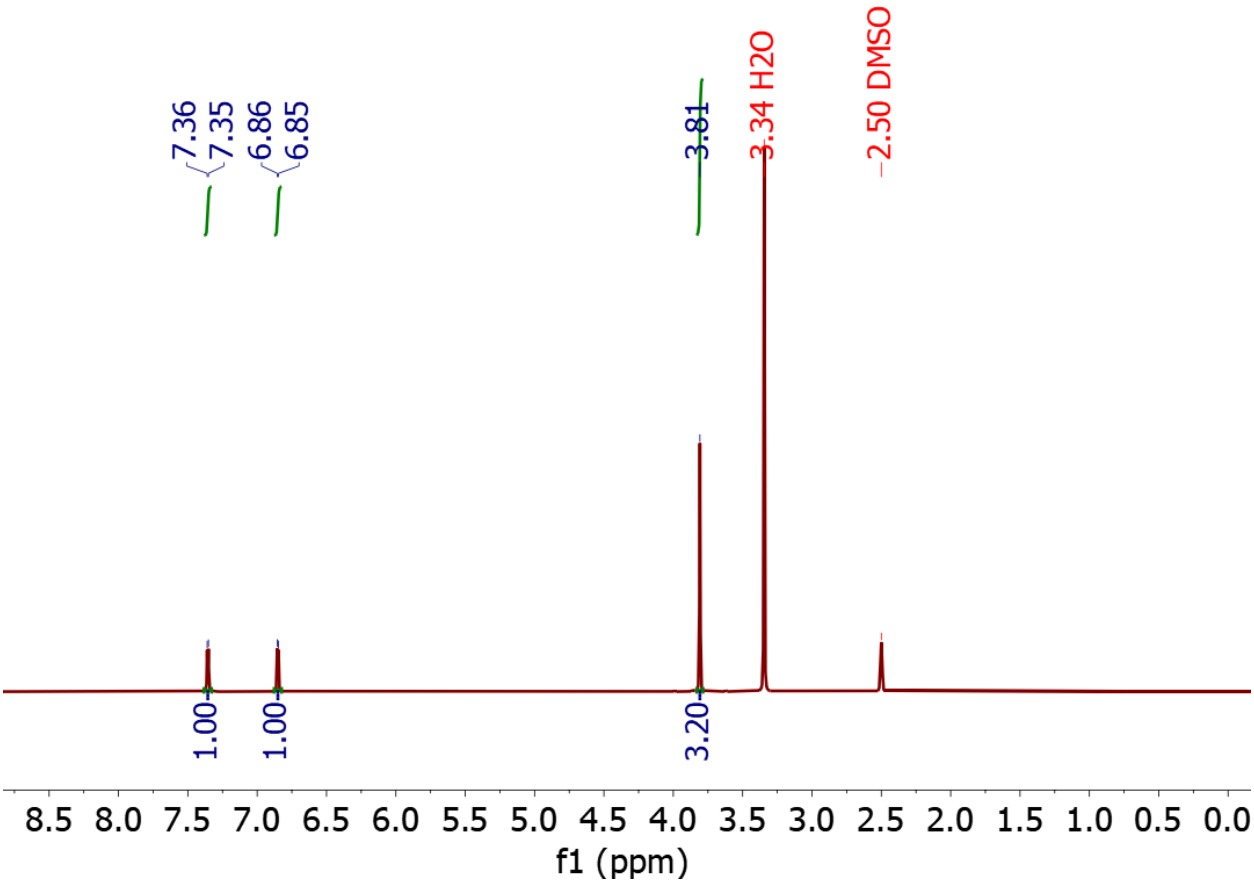

Figure S3. ^{1}H NMR spectrum of synthesized MBFC in DMSO-d_6.

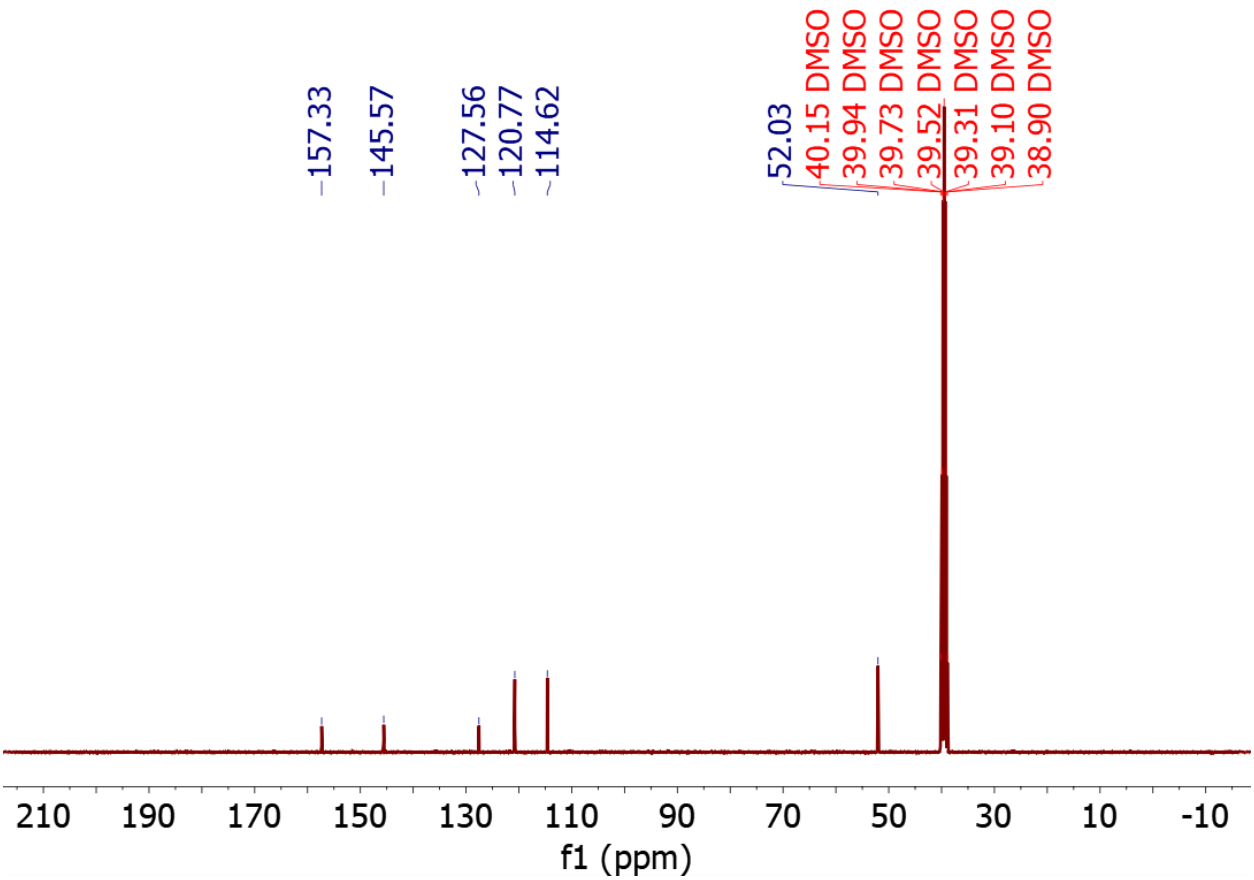

Figure S4. ^{13}C NMR spectrum of synthesized MBFC in DMSO-d_6.

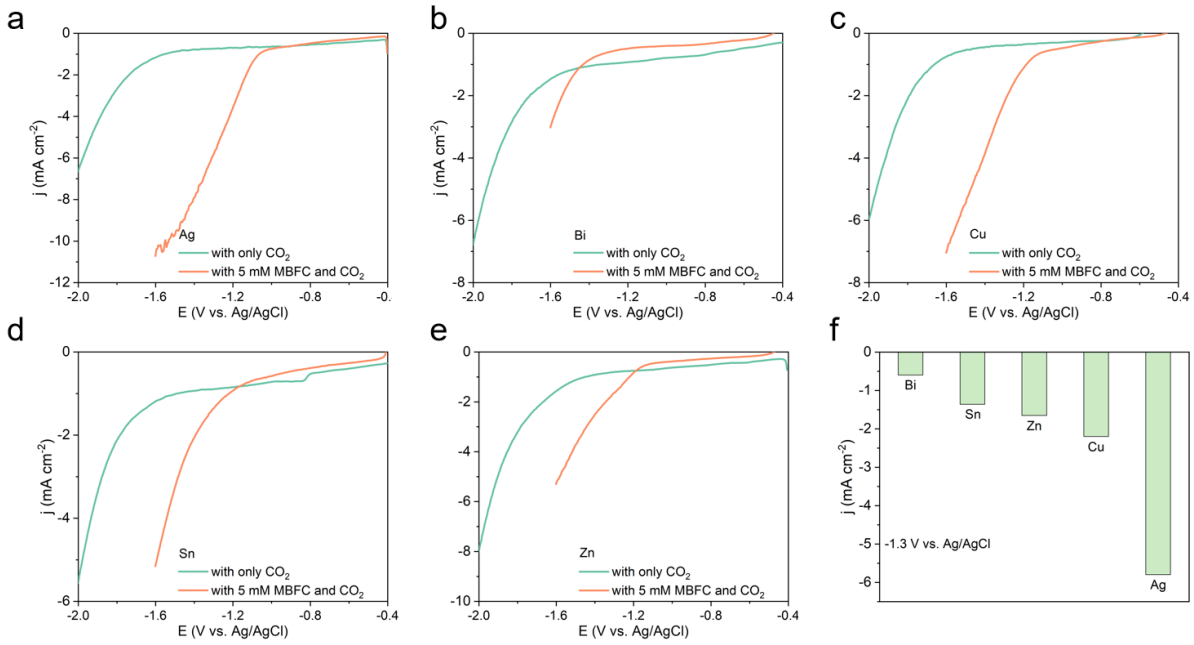

Figure S5. (a)-(e) LSV curves on five different metallic cathodes in 0.1 M TBABr MeCN with a scan rate of 10 mV s^{-1}. (f) Direct comparison of current density obtained on five metallic cathodes at -1.3 V vs. Ag/AgCl.

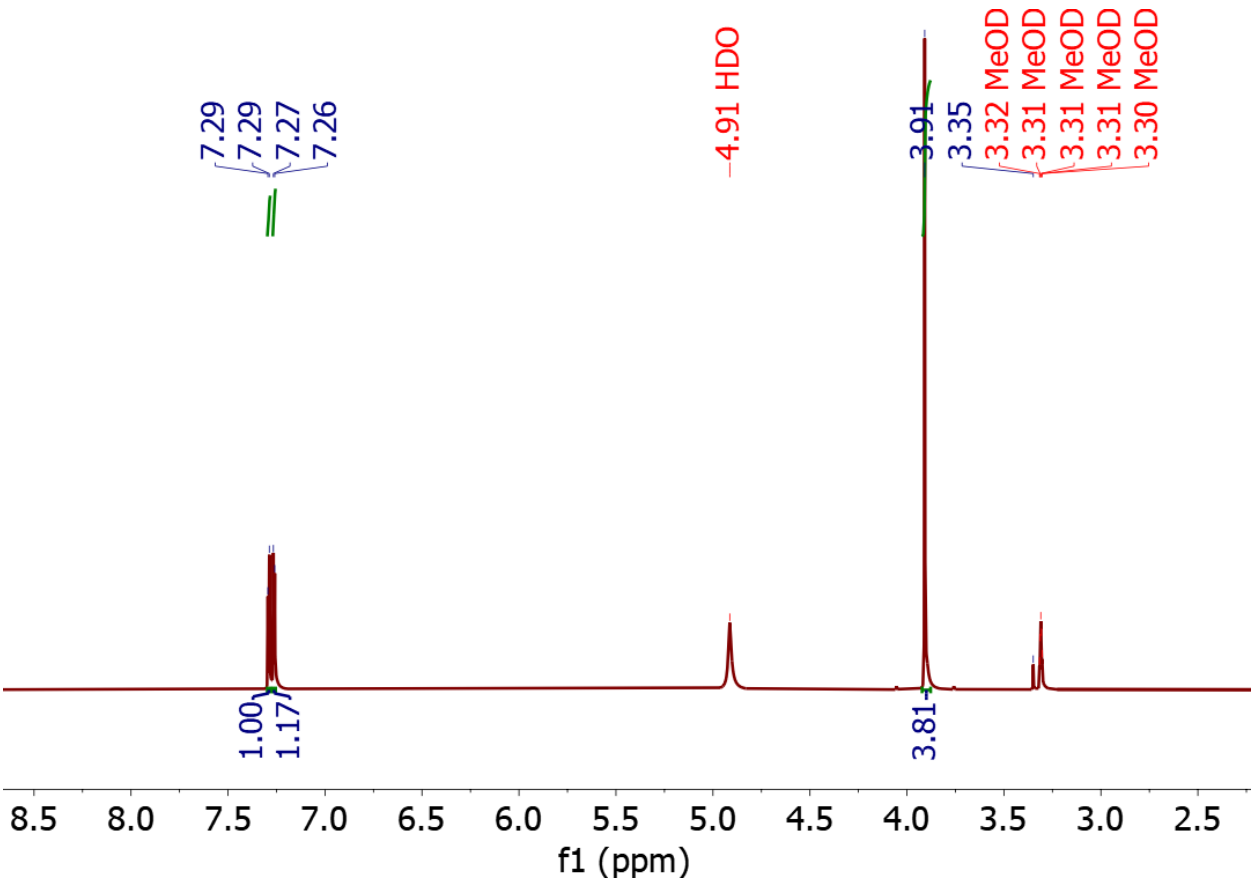

Figure S6. ^{1}H NMR spectrum of synthesized MFCA in Methanol-d_4.

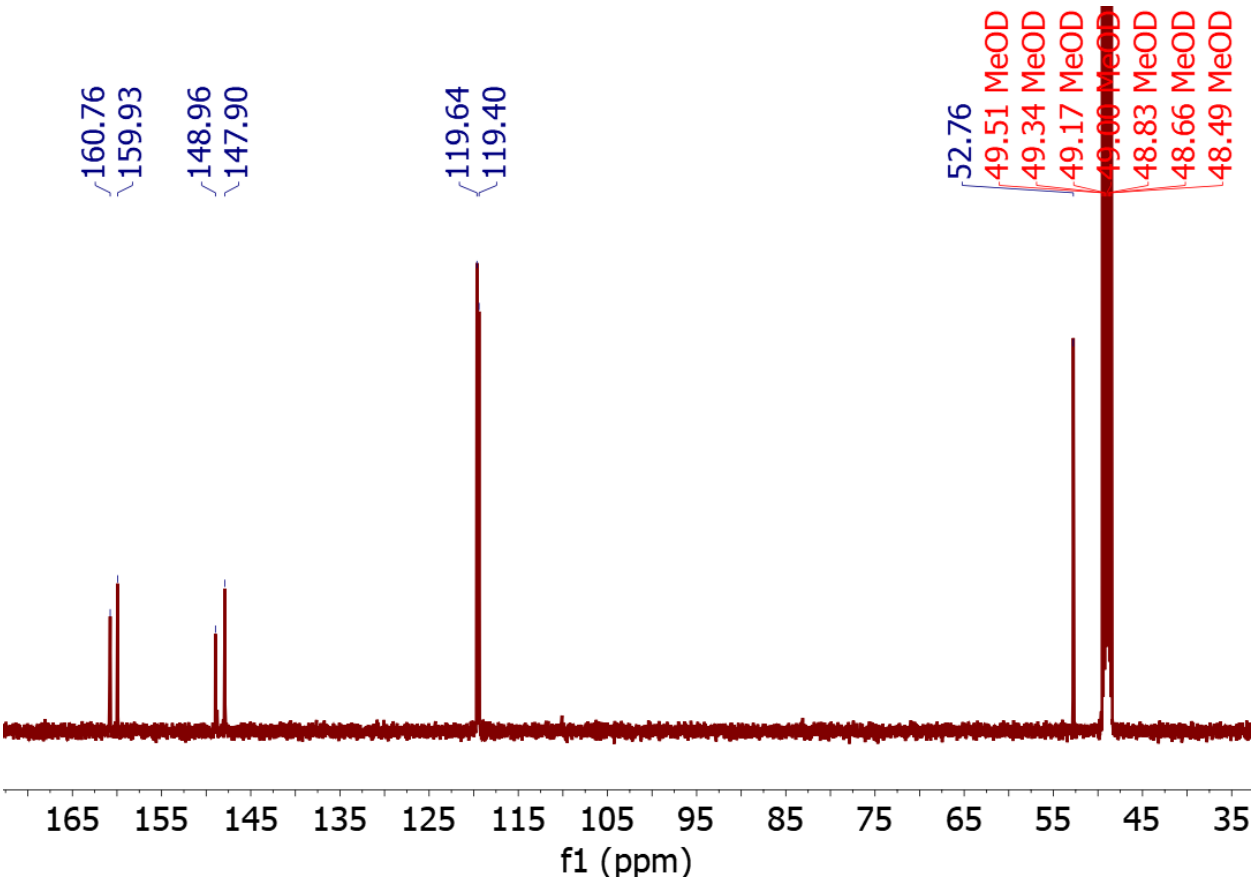

Figure S7. ^{13}C NMR spectrum of synthesized MFCA in Methanol-d_4.

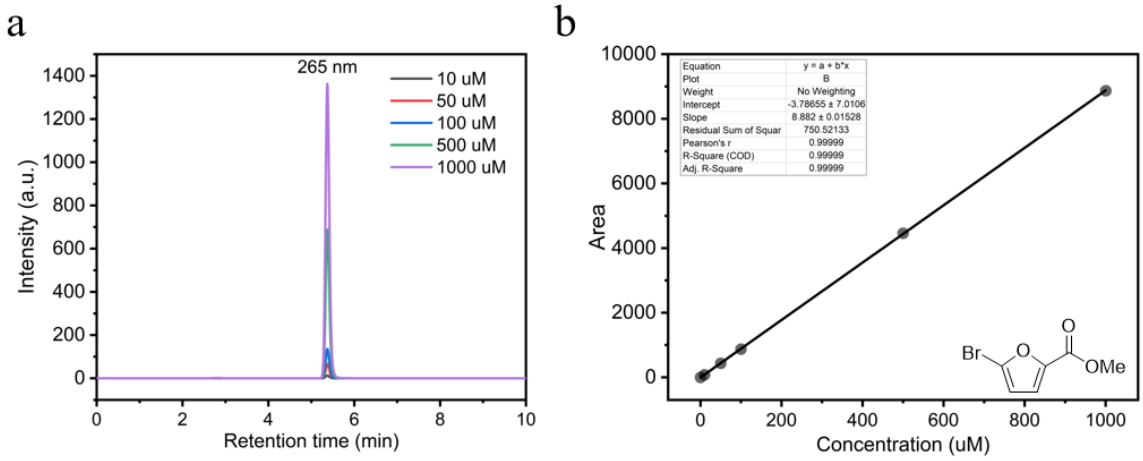

Figure S8. (a) Standard HPLC traces for MBFC substrate. (b) The corresponding calibration curve.

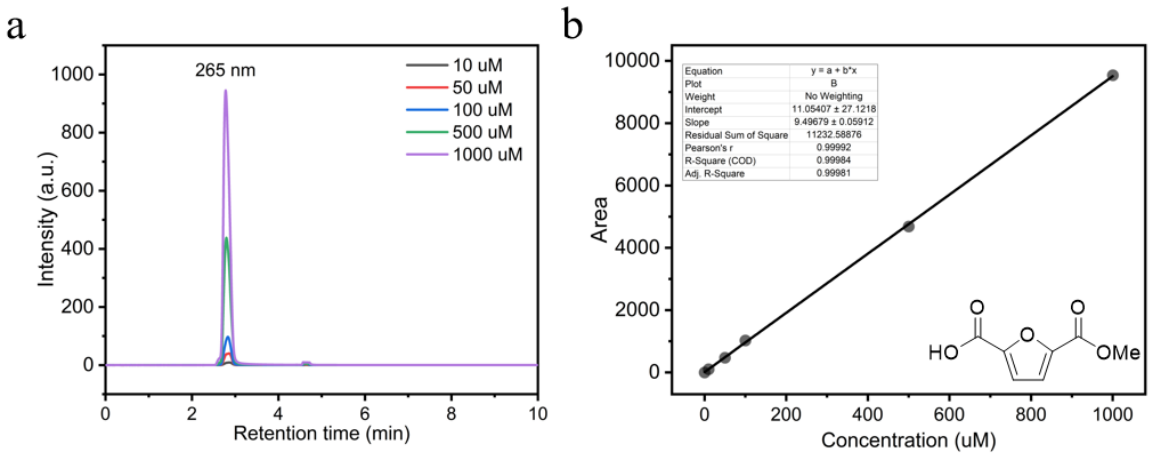

Figure S9. (a) Standard HPLC traces for MFCA product. (b) The corresponding calibration curve.

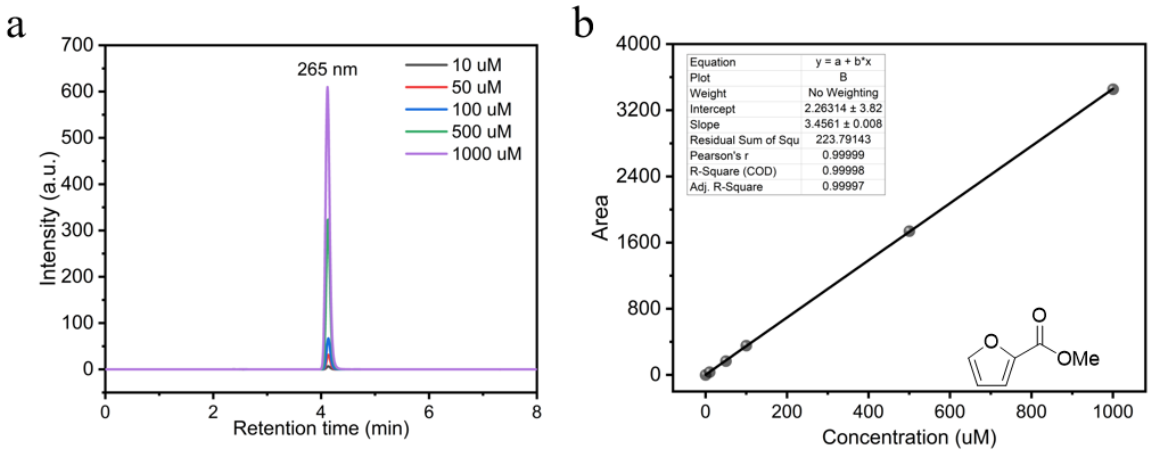

Figure S10. (a) Standard HPLC traces for MF byproduct. (b) The corresponding calibration curve.

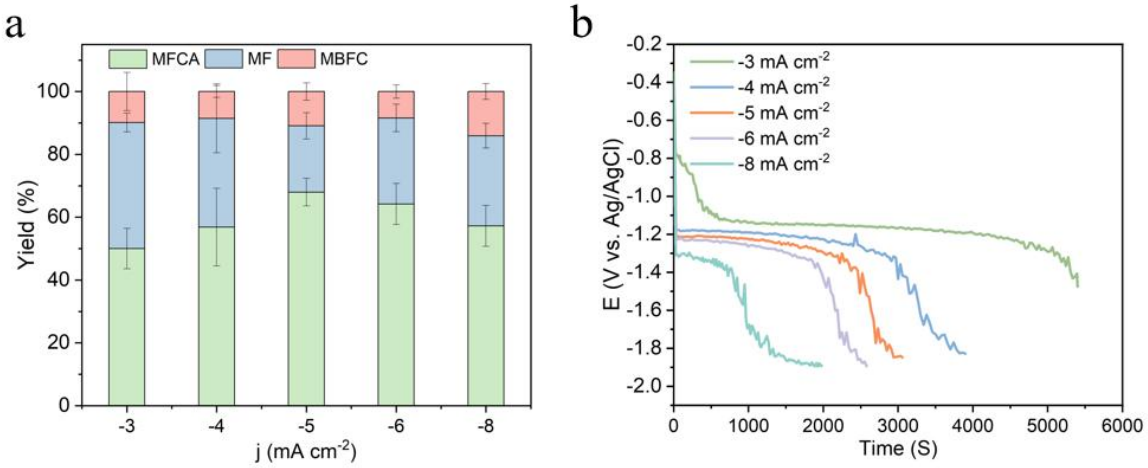

Figure S11. (a) Yield of MFCA, MF and MBFC in 0.1 M TBABr MeCN with 5 mM MBFC at different applied current densities after passing theoretical charge of 14.5 C. (b) Corresponding E-t plots.

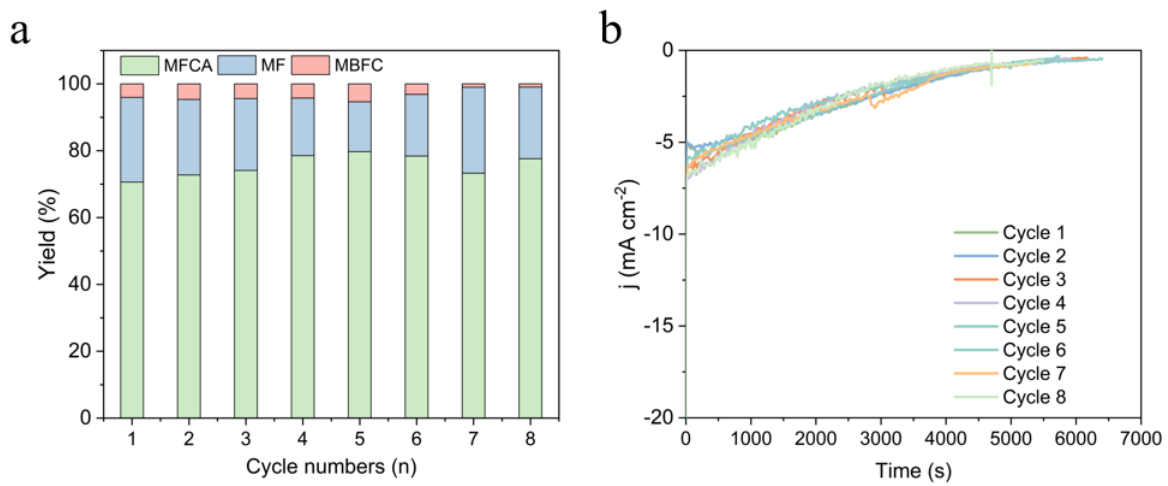

Figure S12. (a) Yield of MFCA, MF and MBFC on the same Ag/CP electrode in 0.1 M TBABr MeCN at -1.4 V vs. Ag/AgCl under eight successive electrolysis cycles. (b) The corresponding it curves.

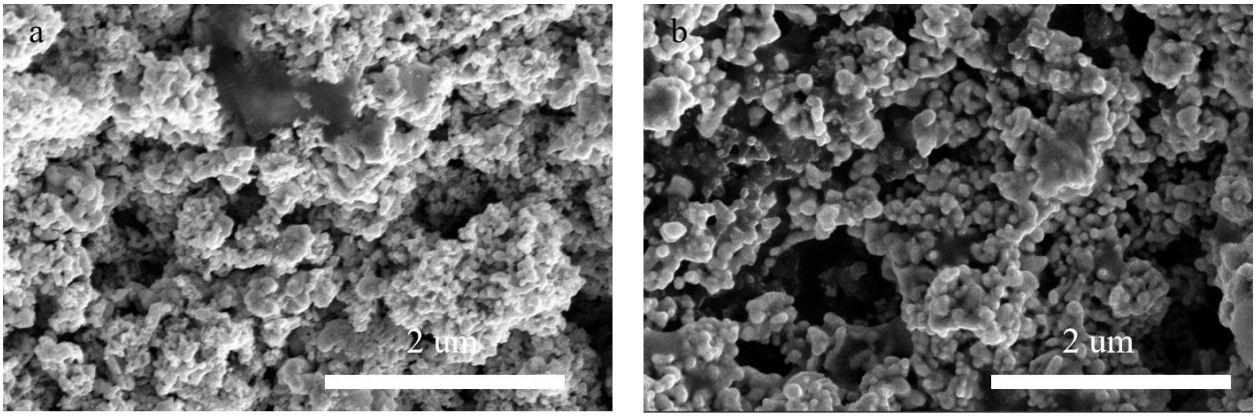

Figure S13. SEM images of Ag/CP catalyst (a) before and (b) after 8 cycles.

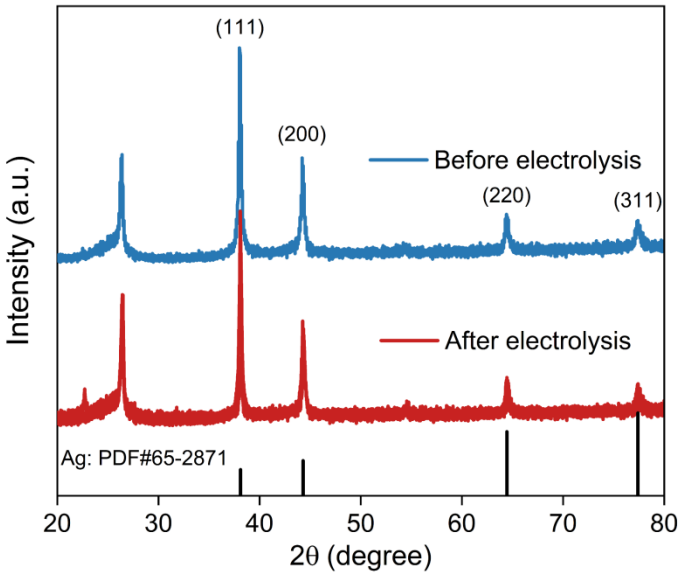

Figure S14. XRD pattern of Ag/CP catalyst before and after 8 cycles.

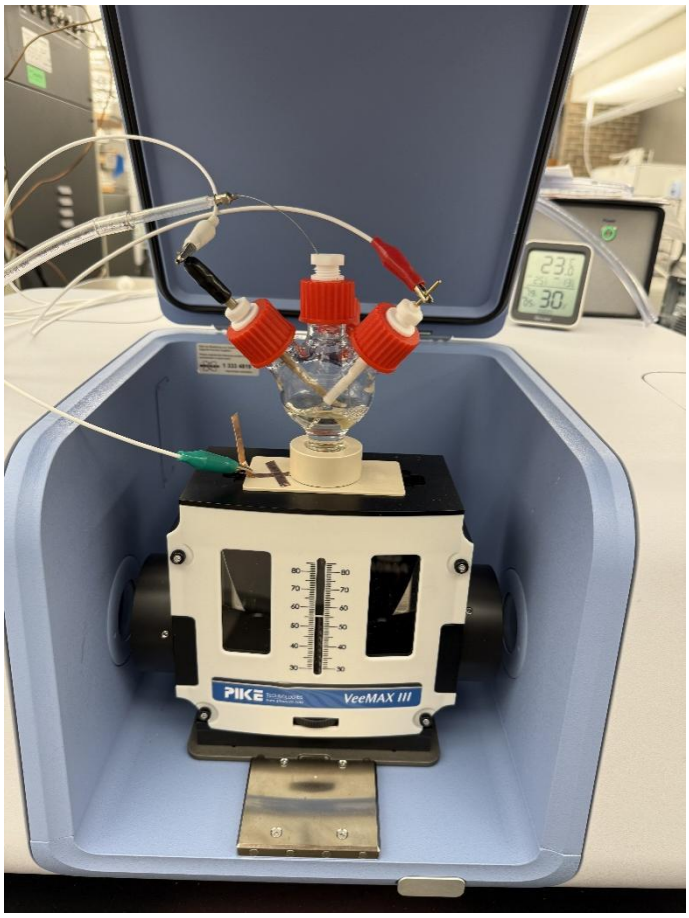

Figure S15. Digital photo of the *in situ* FTIR set up. The working, reference and counter electrodes are Ag on Au coated Si crystal, the leakless Ag/AgCl electrode, and Pt mesh electrode. The yellow color was observed due to the anodic oxidation of bromine anion.

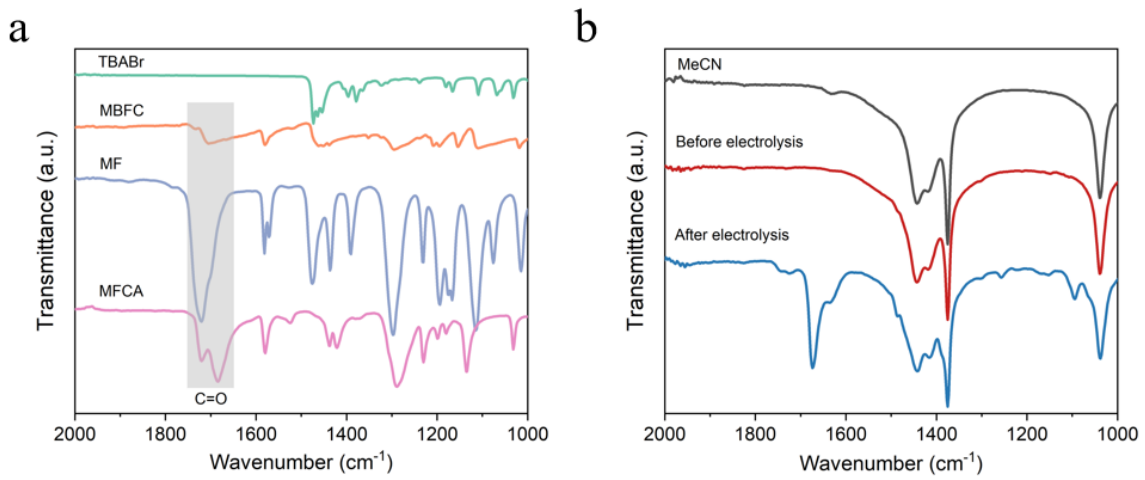

Figure S16. (a) Standard IR spectra of TBABr, MBFC, MF, and MFCA. (b) IR spectrum of pure MeCN and *ex situ* IR spectra obtained before and after electrolysis at -1.4 V vs. Ag/AgCl (the electrolyte after electrolysis has been acidified by 1.5 M HCl).

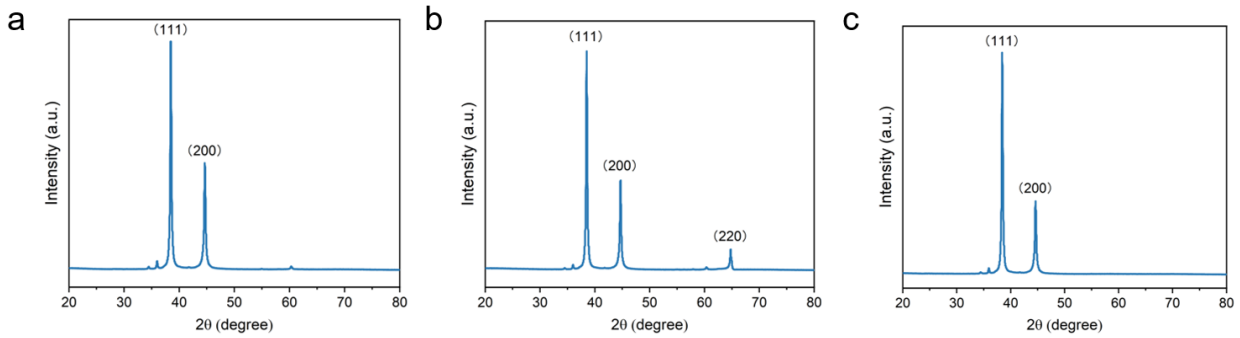

Figure S17. (a)-(c) XRD patterns of single-crystal surfaces of Ag (100), Ag (110), and Ag (111).

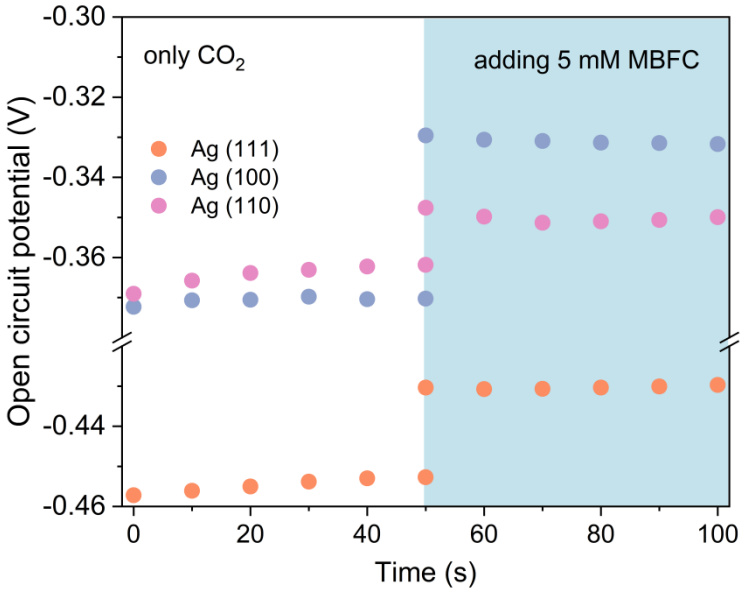

Figure S18. OCP curves of Ag (111), Ag (100), and Ag (110) in CO_2-saturated 0.1 M TBABr MeCN and 5 mM MBFC were added subsequently.

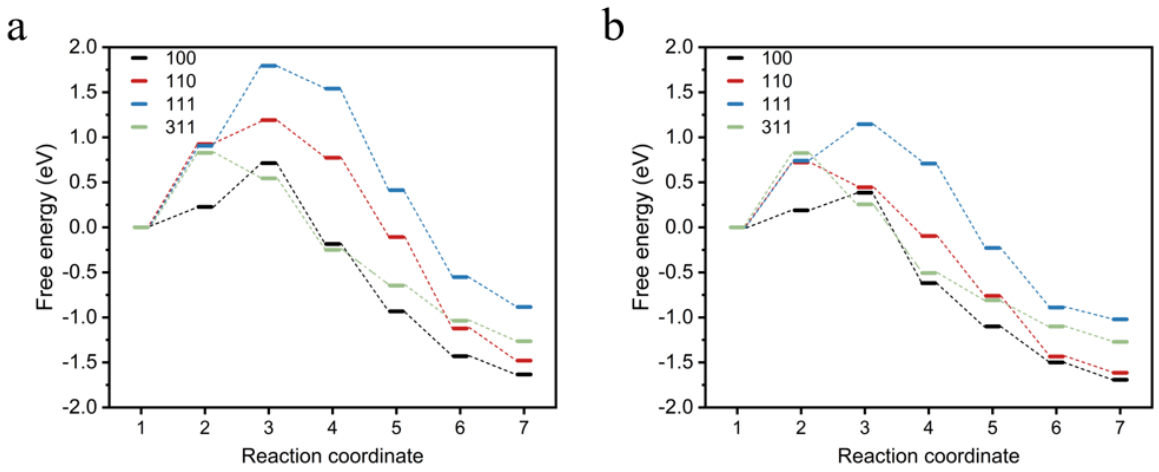

Figure S19. Energy barriers for the debromination of MBFC on Ag facets.

Figure S19a presents the energy barriers obtained from full Cl-NEB calculations performed in VASP using the GGA-PBE+D3 functional with van der Waals corrections. Figure S19b shows the relative energies of the intermediate states computed via single-point VASPsol calculations, representing solvation effects in MeCN. These single-point VASPsol results provide a preliminary idea about facet-dependent activity, indicating that energy barriers are reduced in the MeCN medium. For further analysis, we performed full scale Cl-NEB on Ag-(311) and Ag-(111) facets.

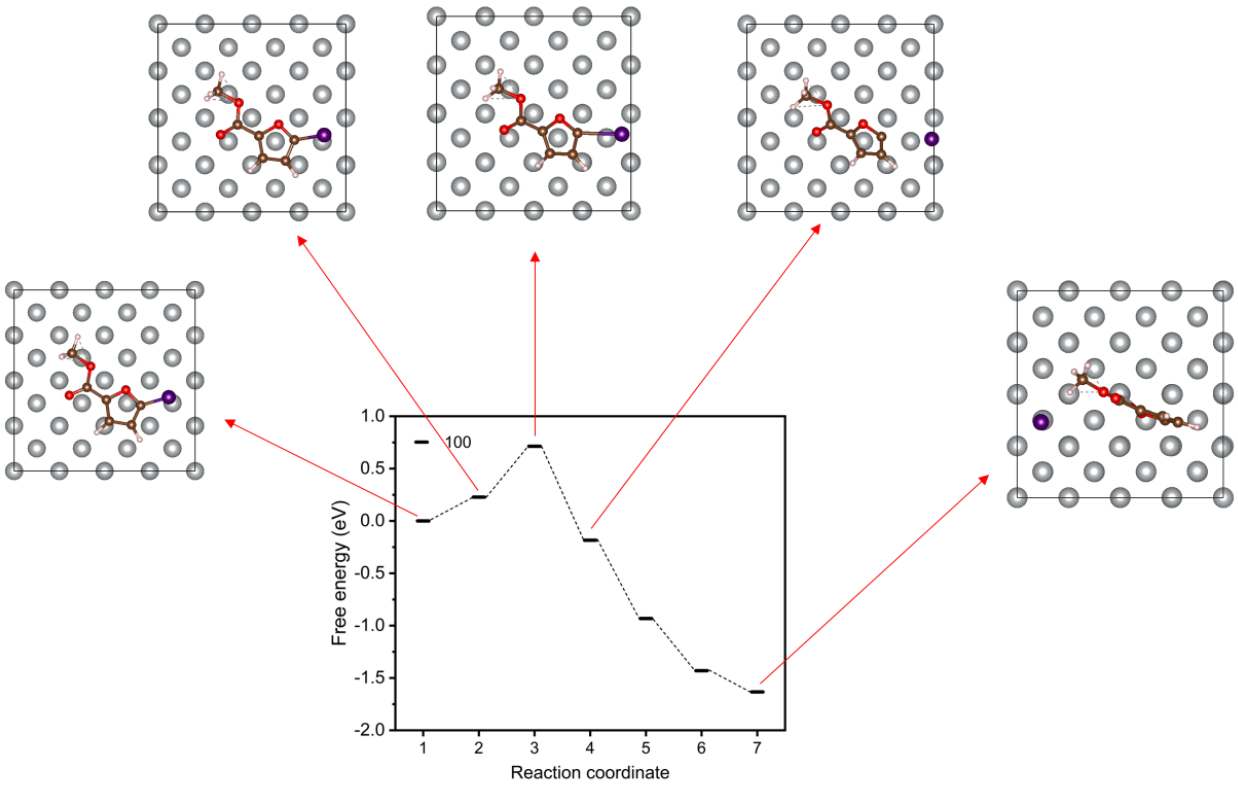

Figure S20. DFT-calculated models of Ag (100) surface and adsorbed intermediates in vacuum.

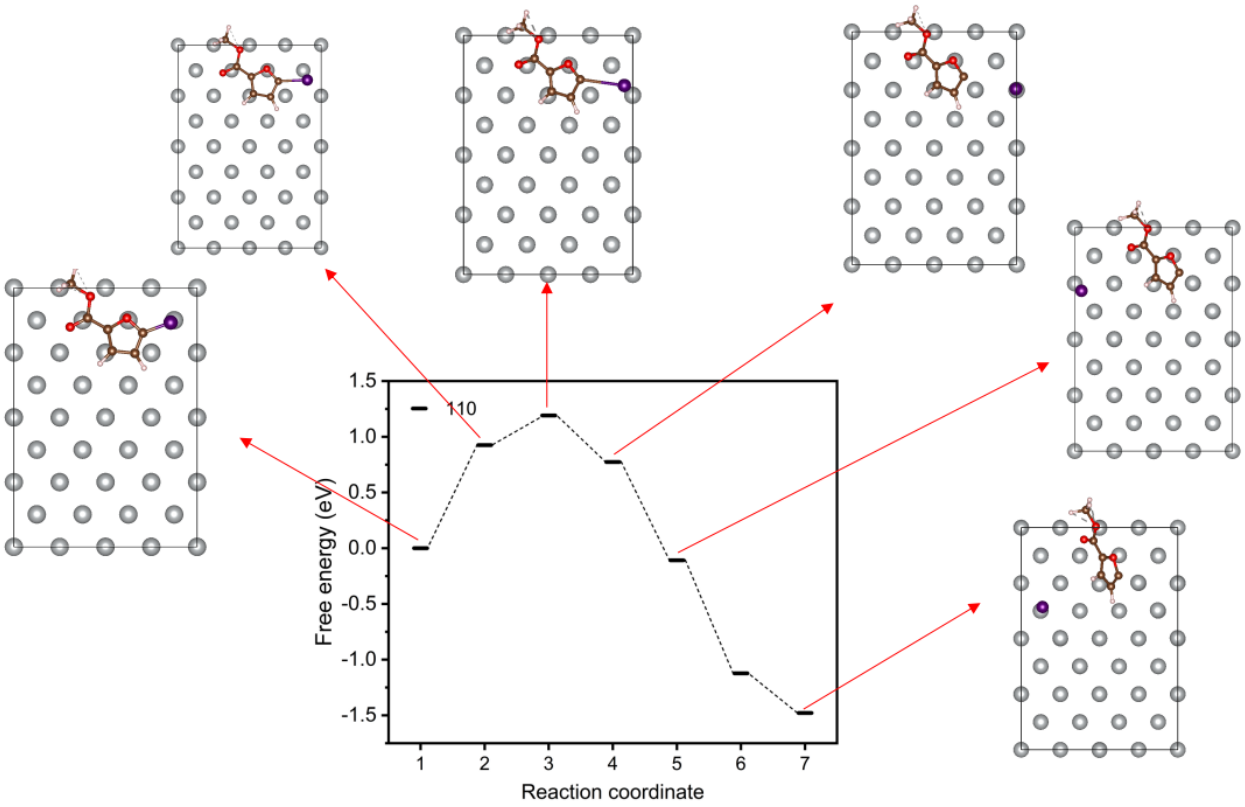

Figure S21. DFT-calculated models of Ag (110) surface and adsorbed intermediates in vacuum.

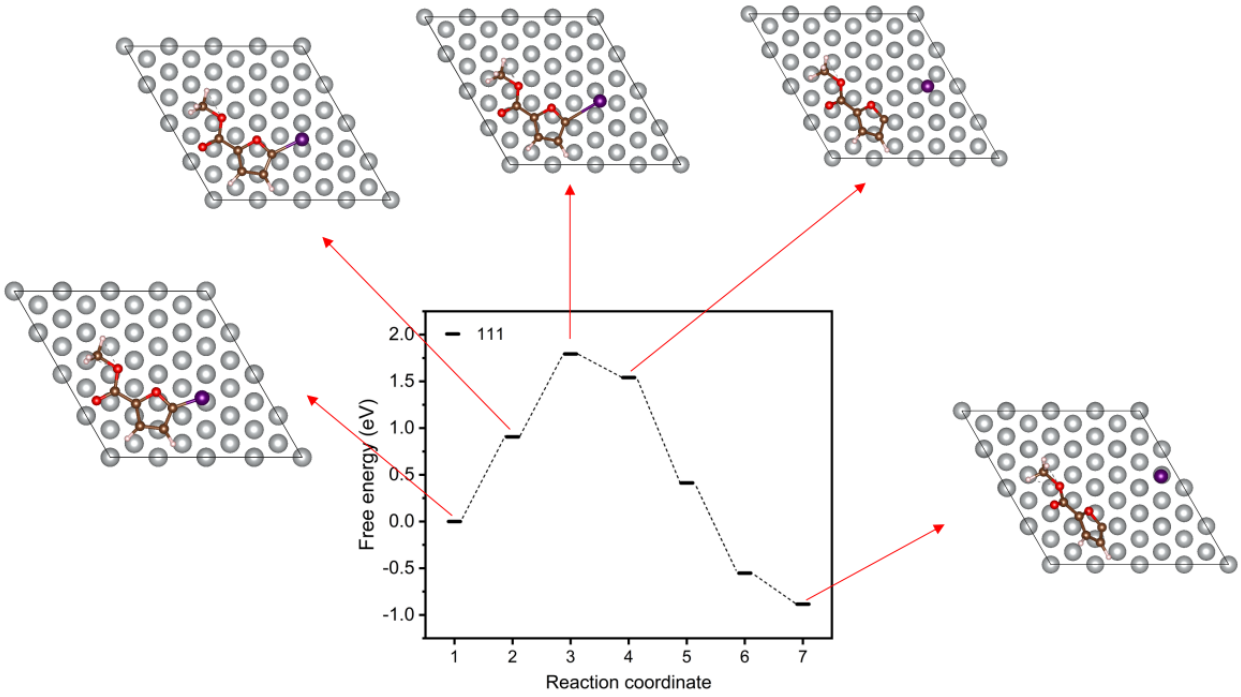

Figure S22. DFT-calculated models of Ag (111) surface and adsorbed intermediates in vacuum.

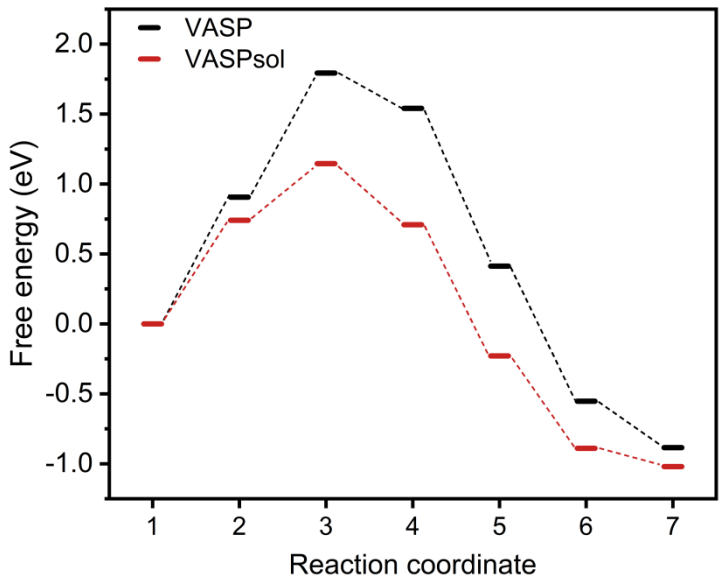

Figure S23. Comparison of DFT-calculated reaction energy diagram for the Ag (111) surface in vacuum and MeCN media from single-point VASPsol++.

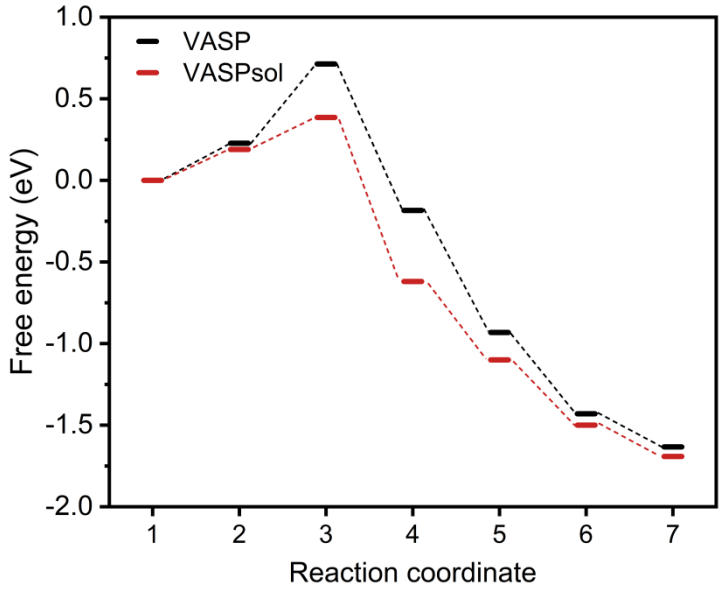

Figure S24. Comparison of DFT-calculated reaction energy diagram for the Ag (100) surface in vacuum and MeCN media from single-point VASPsol++.

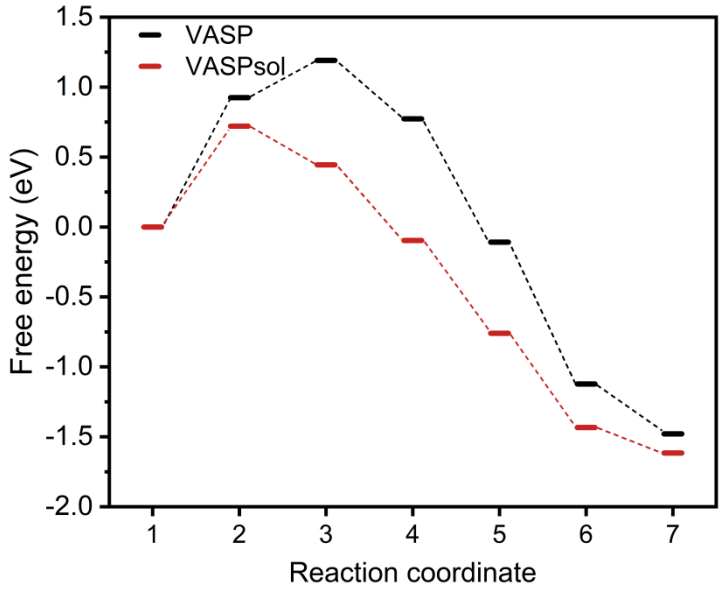

Figure S25. Comparison of DFT-calculated reaction energy diagram over the Ag (110) surface in vacuum and MeCN media from single-point VASPsol++.

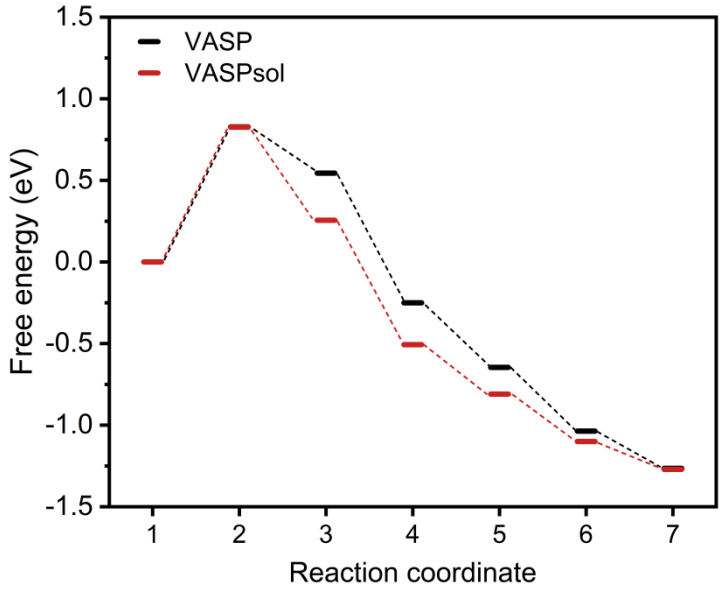

Figure S26. Comparison of DFT-calculated reaction energy diagram for the Ag (311) surface in vacuum and MeCN media from single-point VASPsol++.

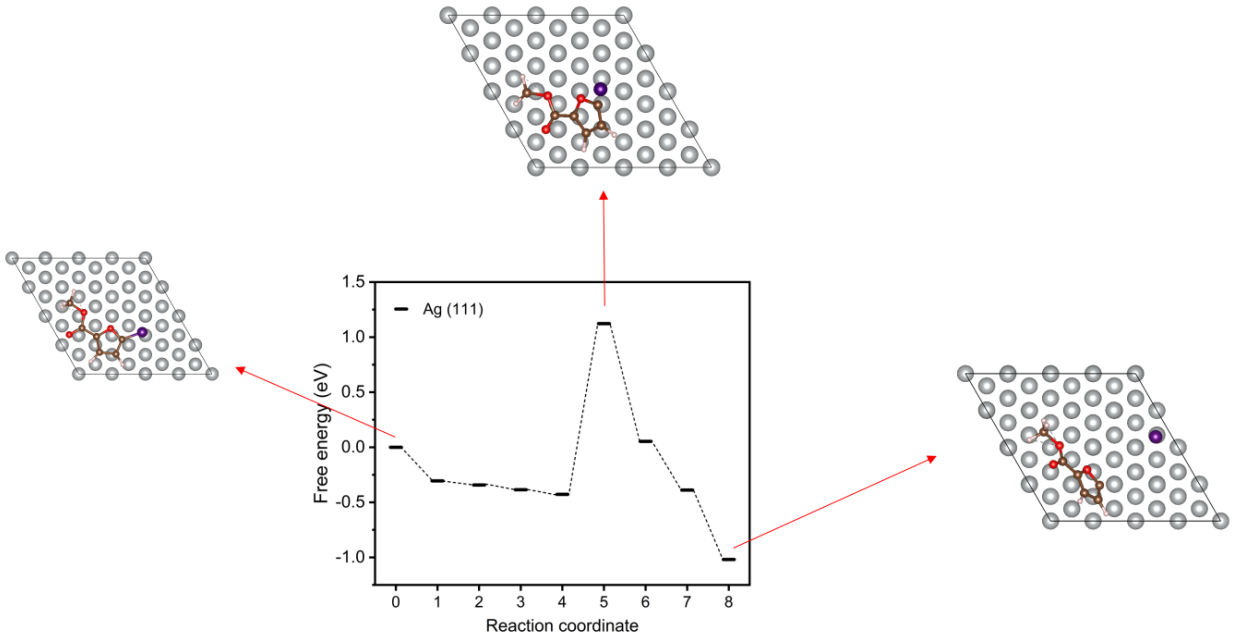

Figure S27. DFT-calculated models of Ag (111) surface and adsorbed intermediates in MeCN from full Cl-NEB calculation in VASPsol++.

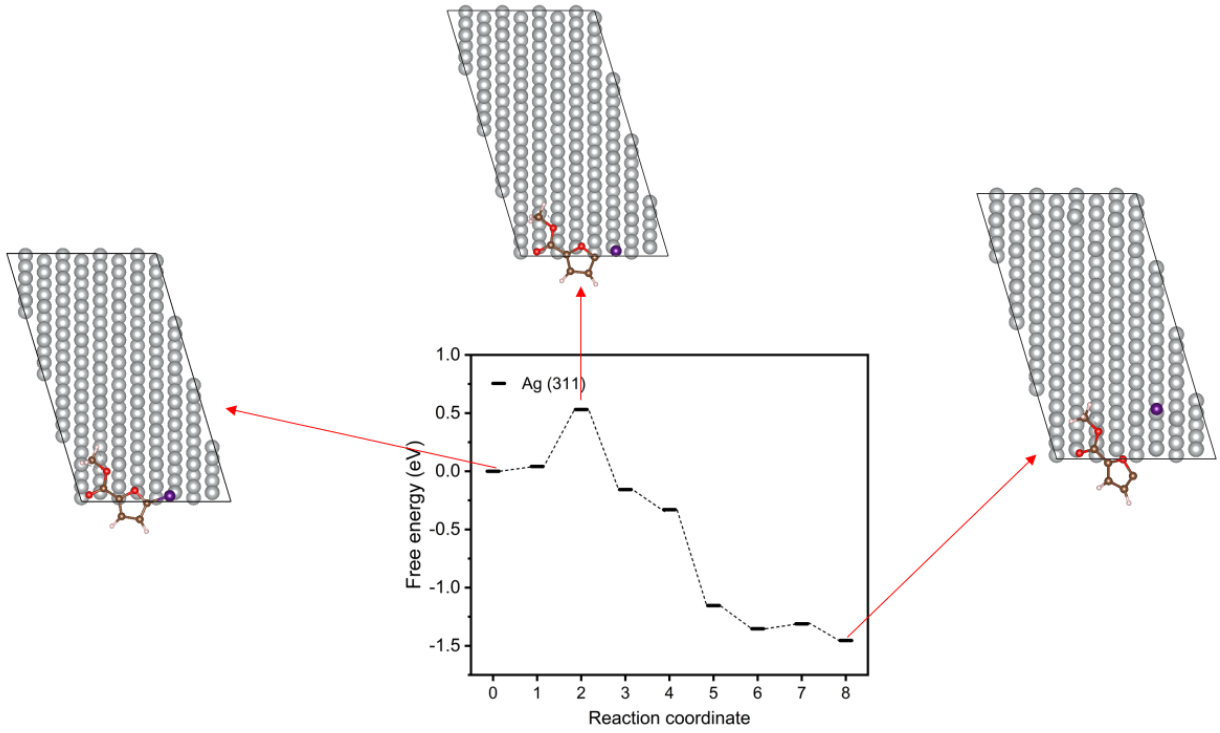

Figure S28. DFT-calculated models of Ag (311) surface and adsorbed intermediates in MeCN from full Cl-NEB calculation in VASPsol++.

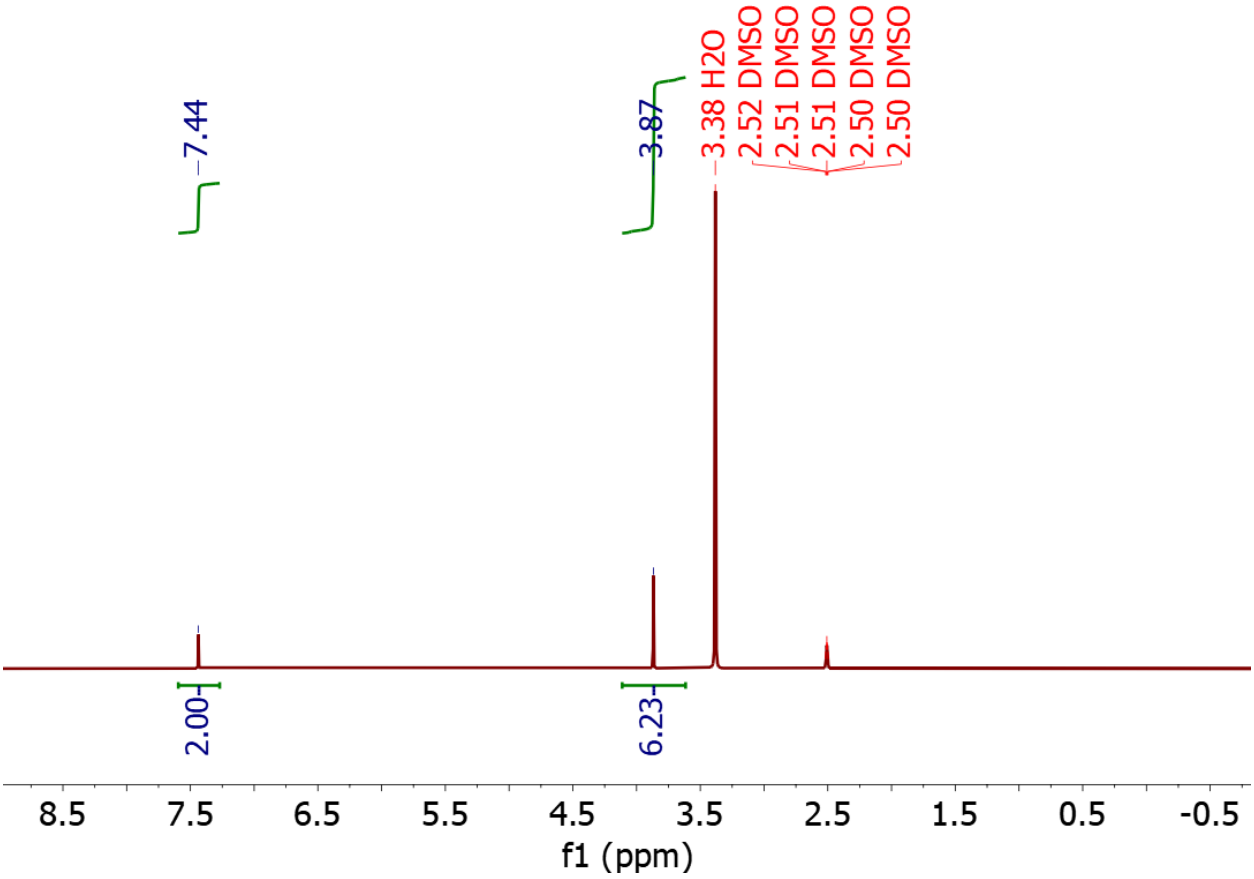

Figure S29. ^{1}H NMR spectrum of synthesized FDME in DMSO-d_6.

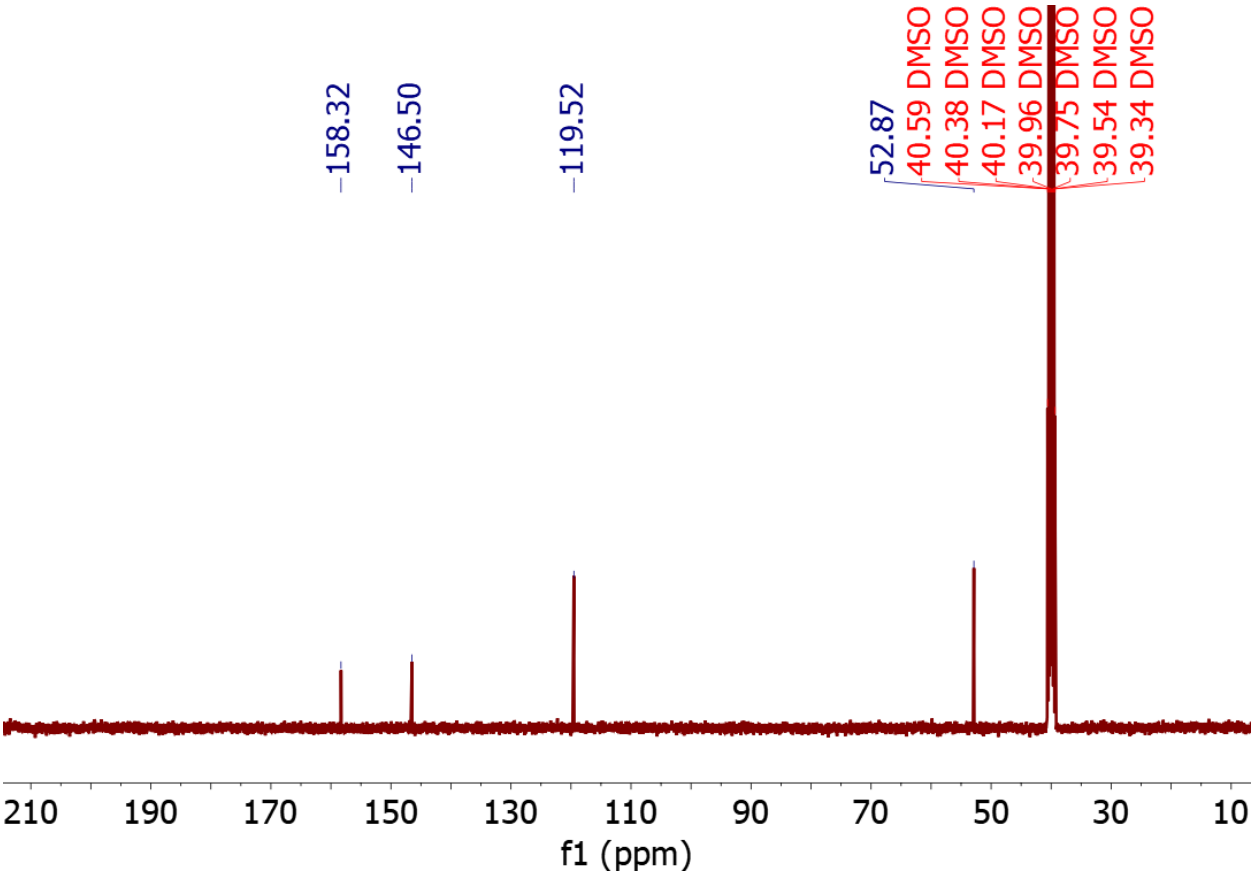

Figure S30. ^{13}C NMR spectrum of synthesized FDME in DMSO-d_6.

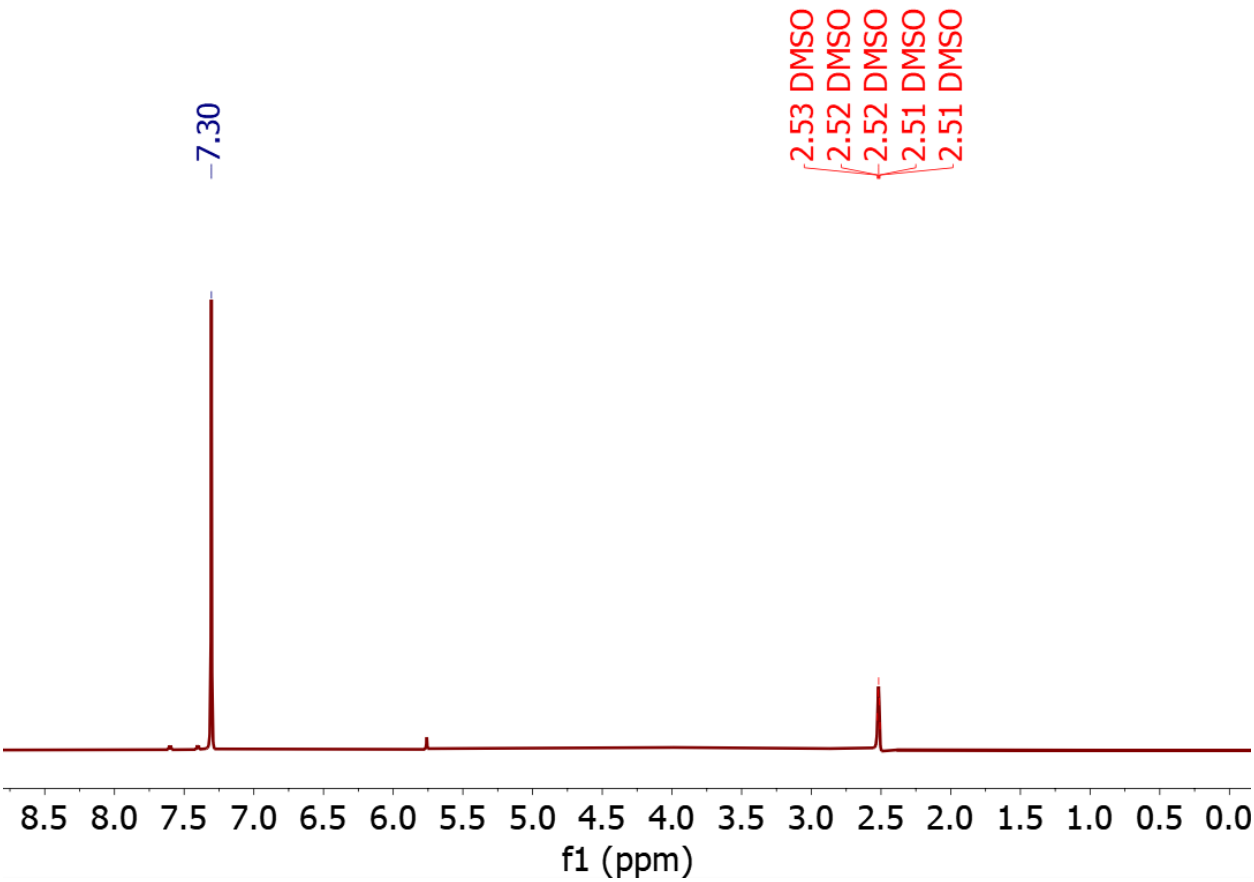

Figure S31. ^{1}H NMR spectrum of synthesized FDCA in DMSO-d_6.

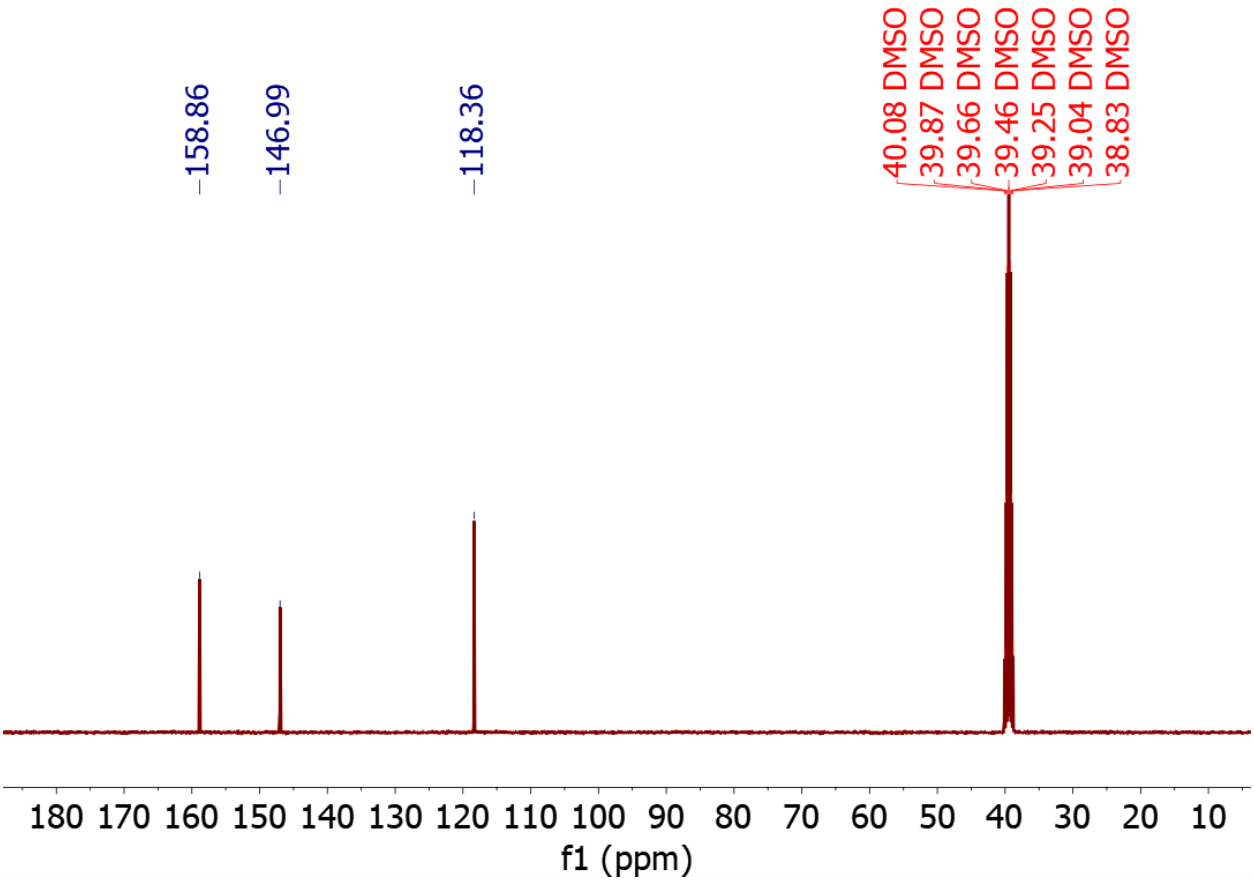

Figure S32. ^{13}C NMR spectrum of synthesized FDCA in DMSO-d_6.

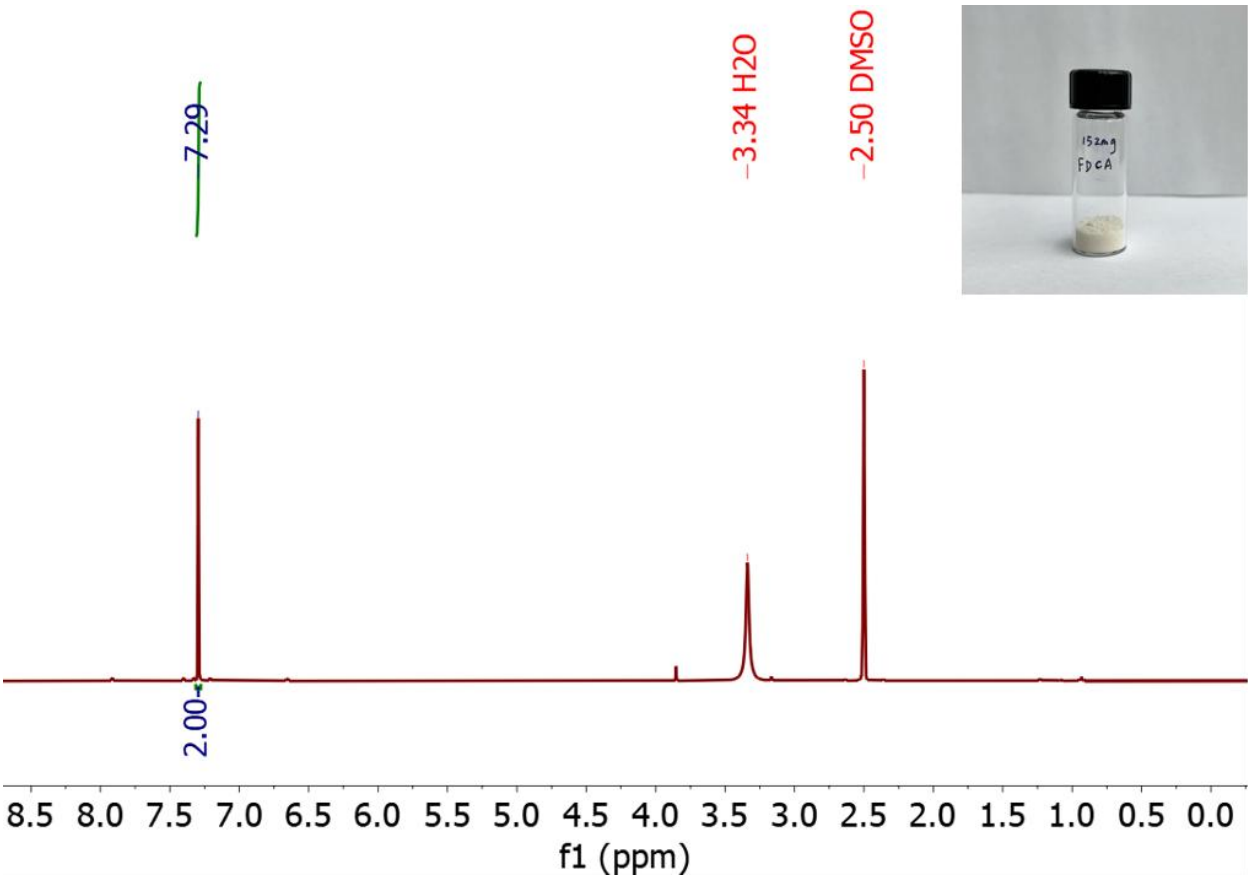

Figure S33. ^{1}H NMR spectrum of electrochemically synthesized FDCA in DMSO-d_6. Inset: digital photo of isolated FDCA from the electrolyte.

Table S1. Summary of the DFT-calculated values for the four different Ag-facets.

Facet	Surface energy (J/m^2)	ΔE_{vacuum} (eV) (VASP)	ΔE_{MeCN} (single-point) (eV) (VASPsol++)	ΔE_{MeCN} (full Cl-NEB) (eV) (VASPsol++)
(100)	1.08	0.72	0.44	N/A
(110)	1.16	1.19	0.73	N/A
(111)	1.02	1.85	1.15	1.13
(311)	1.13	0.85	0.82	0.53

ΔE_{vacuum} refers to full Cl-NEB calculations performed in vacuum using VASP; ΔE_{MeCN} (single-point) refers to single-point VASPsol++ calculations in the MeCN medium, done on top of the vacuum VASP converged structures; and ΔE_{MeCN} (full Cl-NEB) refers to full Cl-NEB calculations in MeCN medium using VASPsol++. From this table, it can be summarized that alongside (200) facet that has been identified from experiments as well as a favorable facet, (311) can also prove to be a promising facet with lower energy barrier for debromination of MBFC. In our DFT calculations we simulated the whole debromination reaction intermediates on the Ag (311) and Ag (111) surface in the MeCN medium.

References

1. J. Deng, H. J. Song, M. S. Cui, Y. P. Du and Y. Fu, *ChemSusChem*, 2014, **7,** 3334–3340.
2. G. Kresse and J. Furthmüller, *Phys. Rev. B*, 1996, **54,** 11169.
3. G. Kresse and D. Joubert, *Phys. Rev. B*, 1999, **59,** 1758.
4. G. Kresse and J. Hafner, *J. Phys.: Condens. Matter*, 1994, **6,** 8245.
5. J. P. Perdew, K. Burke and M. Ernzerhof, *Phys. Rev. Lett.*, 1996, **77,** 3865.
6. J. P. Perdew, A. Ruzsinszky, G. I. Csonka, O. A. Vydrov, G. E. Scuseria, L. A. Constantin, X. Zhou and K. Burke, *Phys. Rev. Lett.*, 2008, **100,** 136406.
7. G. Henkelman, B. P. Uberuaga and H. Jónsson, *J. Chem. Phys.*, 2000, **113,** 9901–9904.
8. S. M. Islam, F. Khezeli, S. Ringe and C. Plaisance, *J. Chem. Phys.*, 2023, **159,** 234117.